the plant journal

SEB SOCIETY FOR EXPERIMENTAL BIOLOGY

The Plant Journal (2023) doi: 10.1111/tpj.16419

MED8 regulates floral transition in Arabidopsis by interacting with FPA

Chen Yuan[1], Yikai Hu[1], Qinggang Liu[1], Jingya Xu[1], Wei Zhou[2], Hao Yu[2,3], Lisha Shen[2,*] and Cheng Qin[1,*]

[1]*College of Life and Environmental Sciences, Hangzhou Normal University, Hangzhou 311121, China,*

[2]*Temasek Life Sciences Laboratory, National University of Singapore, 117604, Singapore, and*

[3]*Department of Biological Sciences, Faculty of Science, National University of Singapore, 117543, Singapore*

Received 18 May 2023; revised 4 July 2023; accepted 31 July 2023.

*For correspondence (e-mail lisha@tll.org.sg; qincheng@hznu.edu.cn).

SUMMARY

Success in plant reproduction is highly dependent on the correct timing of the floral transition, which is tightly regulated by the flowering pathways. In the model plant *Arabidopsis thaliana*, the central flowering repressor *FLOWERING LOCUS C* (*FLC*) is precisely regulated by multiple flowering time regulators in the vernalization pathway and autonomous pathway, including FPA. Here we report that Arabidopsis MEDIATOR SUBUNIT 8 (MED8) promotes floral transition in Arabidopsis by recruiting FPA to the *FLC* locus to repress *FLC* expression. Loss of MED8 function leads to a significant late-flowering phenotype due to increased *FLC* expression. We further show that MED8 directly interacts with FPA in the nucleus and recruits FPA to the *FLC* locus. Moreover, MED8 is indispensable for FPA's function in controlling flowering time and regulating *FLC* expression. Our study thus reveals a flowering mechanism by which the Mediator subunit MED8 represses *FLC* expression by facilitating the binding of FPA to the *FLC* locus to ensure appropriate timing of flowering for reproductive success.

Keywords: MED8, *FLC*, FPA, autonomous pathway, Arabidopsis.

INTRODUCTION

Higher plants typically undergo multiple sequential stages during their life cycle, including seed germination, vegetative growth, reproductive development, embryonic development, and seed maturation. Floral transition, the shift from vegetative growth to reproductive development, is one of the most important developmental transitions in flowering plants. Both genetic and environmental factors influence the floral transition in Arabidopsis. Current studies have shown that there are at least five genetic pathways that regulate this process, including autonomous, vernalization, photoperiod, gibberellin (GA), and thermosensory pathways (Mouradov et al., 2002; Simpson & Dean, 2002; Amasino & Michaels, 2010; Srikanth & Schmid, 2011; Andres & Coupland, 2012).

FLOWERING LOCUS C (*FLC*), a member of the MADS-box family, is considered one of the key regulators of flowering in the flowering regulatory network (He, 2009; Mahrez et al., 2016; Rataj & Simpson, 2014). *FLC* actively inhibits the transcription of regulators of the flowering pathway, including *FLOWERING LOCUS T* (*FT*) and *SUPPRESSOR OF OVEREXPRESSION OF CONSTANS 1* (*SOC1*) (Hepworth et al., 2002; Searle et al., 2006). Several regulators of flowering time in the vernalization and autonomous pathway either accelerate or inhibit the flowering process by directly controlling the expression of *FLC* (He, 2012; Mahrez et al., 2016; Michaels, 2009; Yu & Michaels, 2010). In Arabidopsis, there exist five FLC homologs known as MADS AFFECTING FLOWERING 1–5 (MAF1-5). These MAF1-5 proteins, together with FLC, form a small group of MADS-box proteins that inhibit the initiation of flowering (Kim & Sung, 2010; Parenicova et al., 2003; Ratcliffe et al., 2001; Shen et al., 2014).

The expression of *FLC* is regulated by components of the autonomous promotion pathway. Several genes, including *FLOWERING LOCUS CA* (*FCA*), *FPA*, *FVE*, *FLOWERING LOCUS D* (*FLD*), *LUMINIDEPENDENS* (*LD*), *FY*, and *FLOWERING LOCUS KH DOMAIN* (*FLK*), have been identified as being involved in this pathway (Ausin et al., 2004; He et al., 2003; Hornyik et al., 2010; Kim et al., 2004; Lee et al., 1994; Lim et al., 2004; Macknight et al., 1997; Marquardt, 2006; Mockler et al., 2004; Quesada et al., 2003; Simpson et al., 2003). Autonomous pathway mutants show delayed flowering under both long-day and short-day conditions; however, the delayed flowering can be recovered by vernalization (Abou-Elwafa et al., 2011). Some of these

regulators, including FPA, FCA, and FY, are thought to be involved in the processing of mRNA cleavage and polyadenylation (Hornyik et al., 2010; Liu et al., 2007; Liu et al., 2010; Simpson et al., 2003).

FPA is responsible for encoding a protein that contains three RNA recognition motifs (RRMs) in the N-terminal region, as well as a Spen paralogue and ortholog C-terminal (SPOC) domain (Hornyik et al., 2010; Zhang et al., 2016). It is believed that the SPOC domain facilitates interactions between proteins and has multiple functions within Spen family proteins. The FPA gene was originally discovered as a regulator of flowering time in Arabidopsis (Koornneef et al., 1991). *fpa* mutants exhibit delayed flowering as a result of increased *FLC* expression levels (Schomburg et al., 2001). Furthermore, genome-wide changes in polyadenylation site selection in *fpa* mutant have been analyzed, and the results revealed the chimeric RNA formation between two genes previously thought to be distinct and well-studied in *fpa* mutant (Duc et al., 2013).

Mediator is a transcriptional cofactor complex conserved in all eukaryotes. The transcription complex, consisting of Mediator, RNA polymerase II (RNA Pol II), general transcription factors, and gene-specific transcription factors, is crucial for transcription initiation. The Mediator, first reported in 2007, is composed of 33 subunits in Arabidopsis (Yang et al., 2016). Despite recent progress in the study of plant Mediator subunits in plant growth, abiotic stress, metabolism homeostasis, etc. (Hemsley et al., 2014; Lai et al., 2014; Fallath et al., 2017; Zhang et al., 2018; Wu, Deng, et al., 2020), there is still a significant lack of understanding of the functions of plant Mediator subunits. MEDIATOR SUBUNIT 8 (MED8), one of the subunits that constitute the head module in the Mediator complex, was initially identified as being involved in JA-dependent plant immunity (Kidd et al., 2009). Subsequent investigation revealed that MED8 regulates the plant defense response to *Botrytis cinerea* by interacting with bHLH transcription factor FAMA, which was identified as a critical element in conferring resistance to *Botrytis cinerea*. Further analysis has shown that pathogen resistance regulated by FAMA is dependent on MED8 (Li, Yang, et al., 2018). The tomato *SlMED8* also functions as a regulator of JA-triggered defense responses when encountering fungal pathogen invasion (Zhang et al., 2021). Overexpression of *SlMED8* showed increased tolerance to *Botrytis cinerea*, while *SlMED8* antisense plants demonstrated reduced resistance. Another study showed that MED8 and MED25 had the ability to inhibit short hypocotyl and sugar-responsive gene expression of the *hsr8-1* mutant, which exhibited various sugar hypersensitivity phenotypes (Seguela-Arnaud et al., 2015). Reduced expression of *NtMED8* leads to increased size at multiple levels, ranging from the morphological level to the anatomical, cellular, subcellular, and even organelle ultrastructure level (Wang et al., 2011). Recent studies have shown that MED8 plays a crucial role in recruiting HAC1 and HAC5 (HAC1/5), which are CBP/p300 histone acetyltransferases, to the MEDIATOR complex. They then work together to control flowering time and floral development in Arabidopsis (Guo et al., 2021). Furthermore, MED8 has been shown to regulate oxidative stress responses by inhibiting the expression of genes linked to ROS, jasmonic acid, and defense mechanisms (He et al., 2021). MED8 interacts with NOT2, a transcriptional regulator known as NEGATIVE ON TATA-LESS, to regulate the expression of genes that respond to H_2O_2 and stress. These findings indicate that Arabidopsis MED8 plays various roles in plant growth and stress response. However, molecular mechanisms of MED8's function in Arabidopsis are still largely unclear.

Here, we report the function of MED8 in promoting floral transition in Arabidopsis. We show that MED8 interacts with FPA and facilitates the recruitment of FPA to the *FLC* locus to repress *FLC* expression. Therefore, the MED8-FPA complex plays a critical role in the regulation of *FLC* expression. Our study reveals a molecular mechanism by which MED8 mediates the effect of FPA on a core flowering regulatory network to precisely control the floral transition.

RESULTS

Loss of function of *MED8* delays flowering in Arabidopsis

It has been mentioned that MED8 regulates flowering time (Kidd et al., 2009), thus we proceed to investigate the molecular mechanism by which *MED8* controls the timing of flowering. We first examined the flowering phenotype of the reported *med8* mutant (SALK_092406) (Kidd et al., 2009), which contains a T-DNA insertion in the tenth exon (Figure 1a; Table S1). No *MED8* transcript was detected in *med8* (Figure 1b). Under both long and short day conditions, *med8* mutants exhibited a late-flowering phenotype (Figure 1c,d), suggesting that *MED8* promotes the floral transition regardless of day-length conditions.

To verify that the late-flowering phenotype of *med8* was due to the loss of *MED8* function, we introduced a genomic construct (*gMED8-3FLAG*) into *med8*. This construct contained a 5.2-kb *MED8* genomic region consisting of the 2.4-kb upstream sequence and the 2.8-kb complete coding sequence with introns fused to the 3FLAG tag. Two separate *med8 gMED8-3FLAG* transgenic lines exhibited a flowering phenotype similar to that of wild-type plants (Figure 1e; Figure S1). On the other hand, transgenic plants that overexpress *MED8* exhibited a normal flowering phenotype (Figure S2), indicating that excess amount of *MED8* cannot further accelerate flowering.

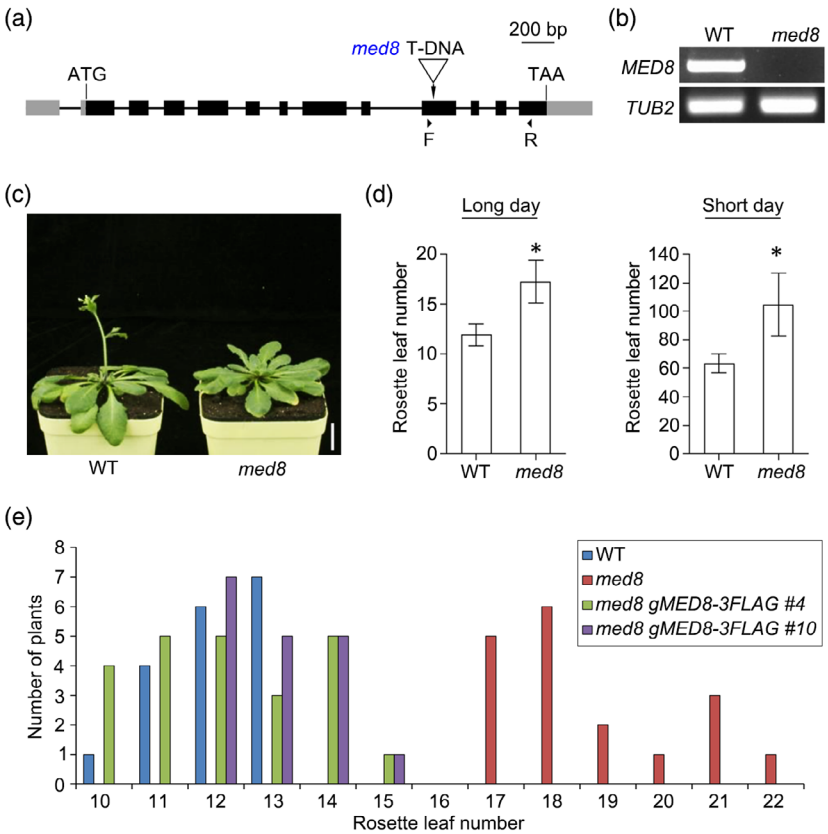

Figure 1. *MED8* regulates flowering time in Arabidopsis.
(a) Schematic diagram shows the *MED8* coding region and the T-DNA insertion site in *med8* (SALK_092406). Exons and untranslated regions are represented by black and gray boxes, respectively, and introns are represented by black lines. Arrowheads indicate the positions of primers used for amplifying the *MED8* transcript as shown in (b). (b) *MED8* transcripts are undetectable in *med8* by semi-quantitative RT-PCR using the primers shown in a. *TUB2* was amplified as an internal control. (c) *med8* shows late flowering under long-day conditions. Scale bar, 1 cm. (d) Flowering time of *med8* grown under long-day and short-day conditions. Values were scored from at least 15 plants of each genotype. Error bars indicate SD. Asterisks indicate significant differences in flowering time between *med8* and wild-type (WT) plants (Student's *t*-test, $P < 0.05$). (e) Distribution of flowering time in two independent transgenic lines carrying the *gMED8-3FLAG* constructs in the *med8* background grown under long-day conditions.

MED8 is expressed ubiquitously in Arabidopsis

To investigate *MED8* expression patterns, we created a *pMED8-GUS* reporter construct by combining the promoter region and start codon of *MED8* with the GUS gene. The GUS staining patterns were similar in almost all *pMED8-GUS* transgenic lines. Further examination of a single representative line revealed that *MED8* was ubiquitously expressed in whole seedlings, including cotyledons, rosette leaves, and shoot apices at approximately 3–11 days after germination under our growth conditions (Figure 2a–f). In roots and open flowers, a GUS signal was also observed (Figure 2g–i), while wild-type seedlings displayed no GUS staining (Figure 2j). The GUS staining pattern was consistent with the quantitative real-time PCR analysis of *MED8* expression in different plant tissues, indicating that rosette leaves had the highest expression (Figure 2k). Meanwhile, *MED8* expression levels in wild-type seedlings grown under long-day conditions showed slight variations in its expression (Figure 2l), which was similar to the *pMED8:GUS* staining pattern (Figure 2a–e). In addition, we examined the MED8 subcellular localization pattern in *35S:MED8-GFP* seedlings and found that MED8-GFP was localized in the nucleus (Figure 2m). The observations indicated that *MED8* may have a constant activity during the growth of Arabidopsis seedlings.

MED8 is mainly involved in the autonomous pathway

Since *MED8* plays a role in the regulation of flowering time, we investigated how these flowering pathways affect *MED8* expression. The level of *MED8* expression showed slight differences in mutants of several key regulators of the photoperiod pathway (Figure 3a). Under long-day conditions, the expression levels of *GI*, *CO*, and *FT* exhibited a diurnal fluctuation, reaching their highest levels at Zeitgeber time (ZT)-8, ZT-0, or ZT-16, respectively (8 h, 0 h, or 16 h after illumination). However, *MED8* expression remained constant throughout the day (Figure S3). These data together with the results of

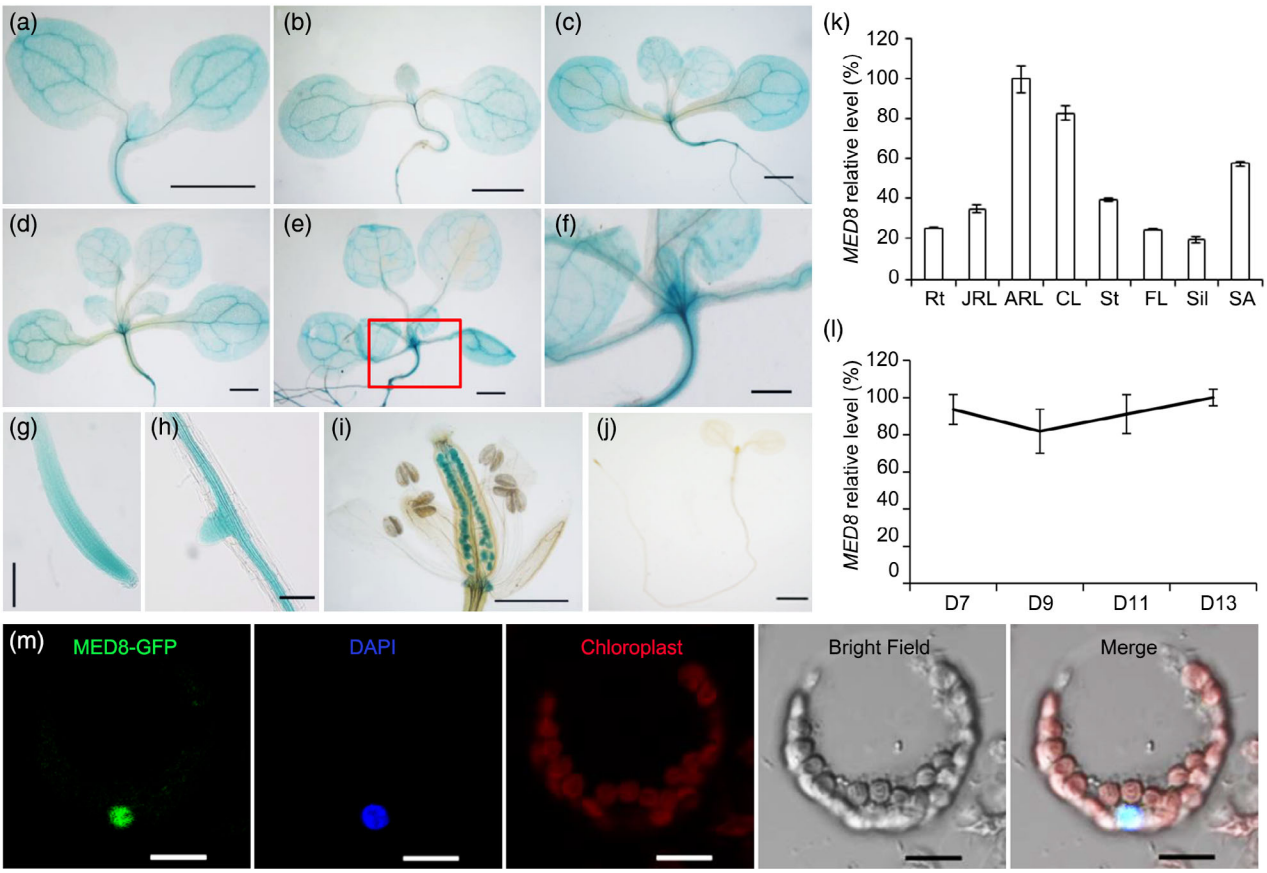

Figure 2. *MED8* is ubiquitously expressed in Arabidopsis.
(a–i) Representative GUS staining of *pMED8:GUS* transgenic plants displays *MED8* expression in seedlings at 3 (a), 5 (b), 7 (c), 9 (d), and 11 (e) DAG, a root tip (g), a primary root (h), and an open flower (i). Scale bars, 1 mm (a–e), 0.1 mm (g), 0.05 mm (h), and 1 mm (i). (f) An enlarged view of a seedling at 11 DAG (e) showing strong *MED8* expression in the shoot apex. Scale bar, 0.5 mm. (j) A negative control of GUS staining with a 3-day-old wild-type seedling. Scale bar, 1 mm. (k) Quantitative real-time PCR analysis of *MED8* expression in various tissues of WT plants. Expression levels are shown as relative values to the maximal level set at 100%. Rt, roots; JRL, juvenile rosette leaves; ARL, adult rosette leaves; CL, cauline leaves; St, inflorescence stems; FL, flowers; Sil, siliques; SA, shoot apices. Error bars indicate SD of three biological replicates. (l) Temporal expression of *MED8* in developing wild-type seedlings (7–13 days old) grown under long-day conditions. Error bars indicate SD of three biological replicates. (m) Subcellular localization of MED8-GFP. GFP localization in protoplasts of *35S:MED8-GFP* transgenic plants. Scale bar, 20 μm.

constant *MED8* expression during seedling development (Figure 2l), and *med8* flowered late under both long-day and short-day conditions (Figure 1c,d), suggest that *MED8* is not regulated by the photoperiod pathway. GA treatment had little effect on *MED8* expression (Figure 3c), indicating that the transcriptional regulation of *MED8* is independent of the GA pathway. The expression of *MED8* was not altered by the vernalization treatment in both wild-type and *FRI FLC* seedlings (Figure 3d), and *med8* displayed a normal response to vernalization (Figure 3e), suggesting that the vernalization pathway did not regulate *MED8*. In addition, the expression of *MED8* was only slightly downregulated as temperature increased from 16°C to 27°C (Figure 3f) within the range of ambient temperature (Wigge, 2013). The absence of *SHORT VEGETATIVE PHASE* (*SVP*), a key component of thermosensory pathway, resulted in a flowering phenotype that was not affected by temperature as reported in previous studies (Pose et al., 2013; Yan et al., 2014) (Figure 3g). In contrast, *med8* exhibited temperature-dependent flowering from 16°C to 27°C similar to wild-type plants (Figure 3g). Consistently, *MED8* expression in *svp-41* or in *35S:SVP* was comparable at 16°C, 23°C, and 27°C (Figure 3f). These findings indicated that *MED8* did not function in the thermosensory pathway.

We further examined *MED8* expression in various mutants of autonomous pathway genes, including *fpa-7*, *fca-2*, *fld-3*, *flk-1*, and *fve-4*. *MED8* expression was not significantly altered in these mutants (Figure 3B). But the results that *med8* mutants exhibited late flowering under both long-day and short-day conditions (Figure 1c,d) and that the late flowering of *med8* could be suppressed by vernalization treatment (Figure 3e), suggested that *MED8* might be involved in the autonomous pathway. Together, these observations suggest that MED8 might be a novel regulator in the autonomous pathway.

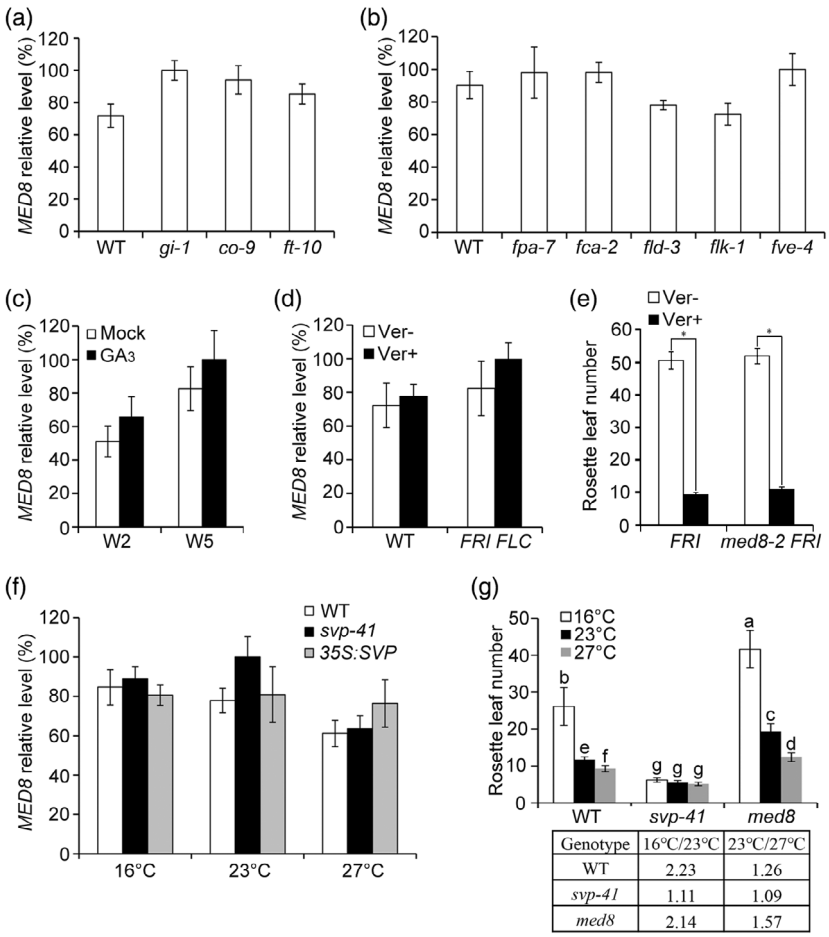

Genotype	16°C/23°C	23°C/27°C
WT	2.23	1.26
svp-41	1.11	1.09
med8	2.14	1.57

Figure 3. Effects of various flowering genetic pathways on *MED8* mRNA expression.
(a) *MED8* expression in photoperiod-pathway mutants at 9 DAG. Gene expression levels in (a–d, f) determined by quantitative real-time PCR were normalized to *TUB2* expression and shown as relative values to the maximal gene expression level set at 100%. Error bars denote SD. (b) *MED8* expression in autonomous-pathway mutants at 9 DAG grown under long-day conditions. (c) Effect of GA treatment on *MED8* expression. For GA treatment, 2-week-old wild-type plants grown under short-day conditions were applied weekly with exogenous GA (100 μM) or 0.1% ethanol (Mock). Seedlings treated for 2 weeks (W2) or 5 weeks (W5) were harvested for expression analysis. (d) Effect of vernalization treatment on *MED8* expression. For vernalization treatment, seeds were grown on Murashige and Skoog medium and vernalized at 4°C under low light conditions for 8 weeks. Nine-day-old seedlings grown under long-day conditions were harvested for expression analysis. (e) Flowering time of *FRI* and *FRI med8* plants in response to vernalization treatment under long-day conditions. (f) *MED8* expression in wild-type, *svp-41*, and *35S:SVP* grown at 16°C, 23°C and 27°C. Nine-day old seedlings grown under long-day conditions were harvested for expression analysis. (g) Flowering time of wild-type, *svp-41*, and *med8* grown at 16°C, 23°C and 27°C under long-day conditions. The ratios of flowering time between 16°C and 23°C (16°C/23°C) and between 23°C and 27°C (23°C/27°C) for all the genotypes are indicated in the attached table. Values were scored from at least 20 plants of each genotype. Error bars indicate SD. Expression analysis was performed with three biological replicates ($P < 0.05$, two-way ANOVA).

MED8 promotes flowering by repressing *FLC*

To further understand the effect of *MED8* on flowering time, we identified potential targets of *MED8* that could potentially account for its role in promoting flowering. We first performed transcriptomic analyses of wild-type and *med8* mutant seedlings by RNA-seq. In comparison with wild-type plants, 956 genes that were differentially expressed (DEGs) were identified in *med8* mutants. Among them, 474 genes were up-regulated and 482 genes were down-regulated in *med8* mutants (Figure S4; Dataset S1). According to gene ontology (GO) analysis, the genes that were up-regulated and down-regulated in *med8* mutants were enriched in various biological processes, including systemic acquired resistance, defense response, response to oomycetes, response to fungus, response to bacterium, response to jasmonic acid, cellular response to hypoxia (Figure S4), consistent with previous observations (Hammoudi, 2021; Wang et al., 2011; Xu & Li, 2012; Zhang et al., 2021).

Consistent with the delayed flowering phenotype of *med8*, many flowering-related genes were misregulated in *med8* mutants (Dataset S2). Briefly, flowering repressing gene *FLC* was upregulated, whereas the expression of flowering-promoting genes like *FT*, *TWIN SISTER OF FT* (*TSF*), and *SOC1* was decreased, suggesting that these flowering time genes might contribute to the late flowering of *med8* mutants.

To confirm the expression of the DEGs associated with flowering time that were identified by RNA-seq, we examined the temporal expression of various key flowering time regulators in wild-type and *med8* seedlings. We observed a significant increase in the expression of *FLC*, the key flowering repressor, in *med8* mutants compared to wild-type seedlings (Figure 4a). On the other hand, expression of *FT* and *SOC1*, two key regulators of the flowering pathway downstream of *FLC*, was decreased in developing *med8* seedlings (Figure 4b,c), consistent with the late-flowering phenotype of *med8*. Meanwhile, expression levels of *MAF4* and *MAF5*, two homologs of *FLC*, were increased in *med8* seedlings (Figure S5a,b), whereas expression of *SVP*, a repressor of *FT* and *SOC1*, remained unchanged in *med8* (Figure S5c). In addition, expression levels of autonomous pathway genes were not altered in *med8* mutants (Dataset S3).

We then examined genetic interactions among *MED8*, *FLC*, *FT*, and *SOC1*. In line with previous studies, *flc-3* exhibited an early flowering phenotype compared to wild-type. The delayed flowering phenotype of *med8* was largely alleviated by *flc-3* under both long-day and short-day conditions (Figure 4d,e; Figure S6), implying that upregulation of *FLC* was mainly responsible for the delayed flowering of *med8*. The late-flowering phenotype of *med8* was enhanced by both *ft-10* and *soc1-2* (Figure S7). Furthermore, we observed that the expression levels of *FT* and *SOC1* in *flc-3 med8* double mutants were similar to those in *med8* mutants (Figure 4f), implying that MED8 regulates *FT* and *SOC1* expression at least partially through *FLC*. We also crossed *med8* with Col plants carrying a functional FRIGIDA (FRI) allele, which expressed high *FLC* levels. *FRI med8* showed a similar flowering time to *FRI* (Figure 4d), indicating that *MED8* functions in the same pathway as *FRI*. These genetic analysis data, together with the expression analysis (Figure 4a–c), demonstrate that MED8 promotes flowering through repressing *FLC* expression.

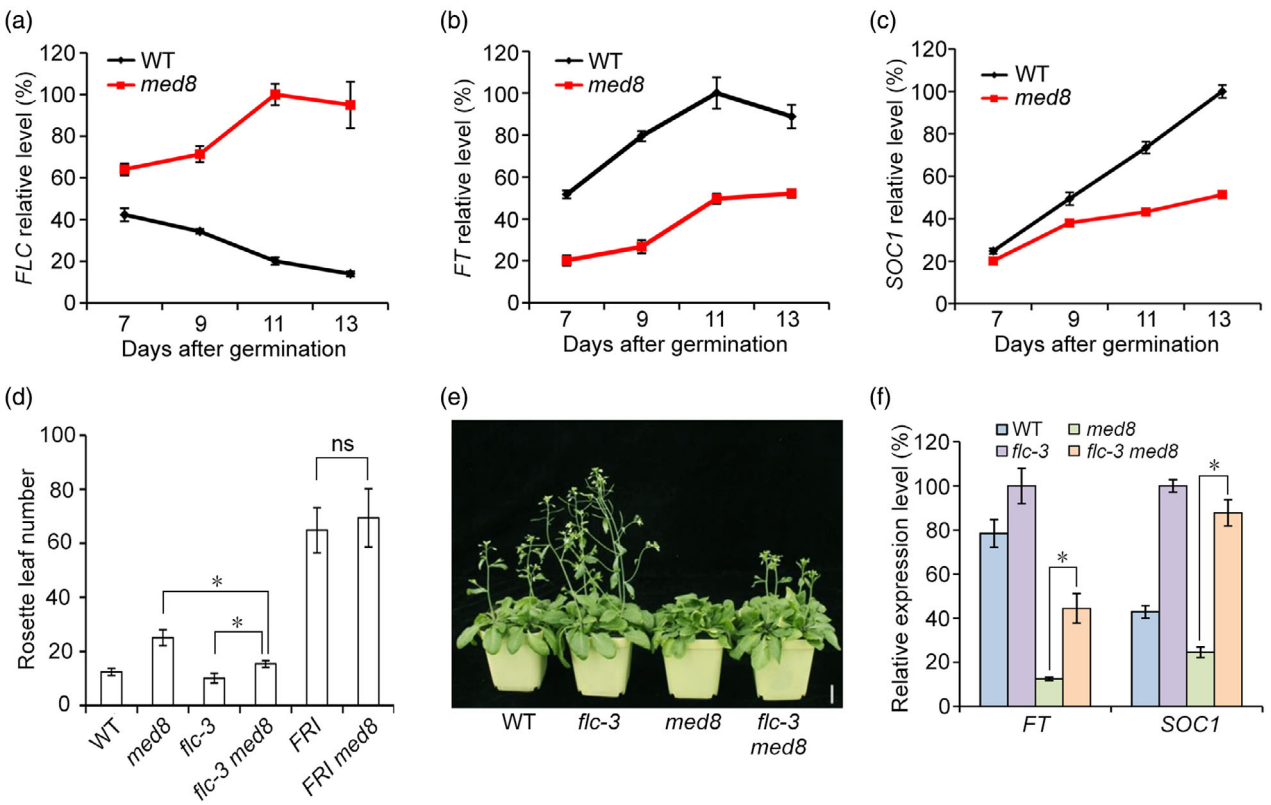

Figure 4. MED8 represses *FLC* expression.
(a–c) Temporal expression of *FLC* (a), *FT* (b), and *SOC1* (c) in developing wild-type (WT) and *med8* seedlings grown under long-day conditions as determined by quantitative real-time PCR. All samples were collected at the end of long-day conditions (ZT16). The levels of gene expression normalized to *TUB2* expression are shown as relative values to the maximal expression level set at 100%. Error bars indicate the SD of three biological replicates. (d) Flowering time of various mutants grown under long-day conditions. Values were scored from at least 15 plants of each genotype. Error bars indicate SD. Asterisks indicate significant differences in flowering time between *med8* and *flc-3 med8* plants, *flc-3* and *flc-3 med8* plants (Student's *t*-test, $P < 0.05$). (e) *med8 flc-3* shows comparable flowering time to wild-type under long-day conditions. Scale bar, 2 cm. (f) Expression levels of *FT* and *SOC1* in WT, *flc-3*, *med8* and *med8 flc-3*. Error bars indicate SD of three biological replicates. Asterisks indicate significant differences in expression levels of *FT* and *SOC1* between *flc-3* and *flc-3 med8* plants (Student's *t* test, $P < 0.05$).

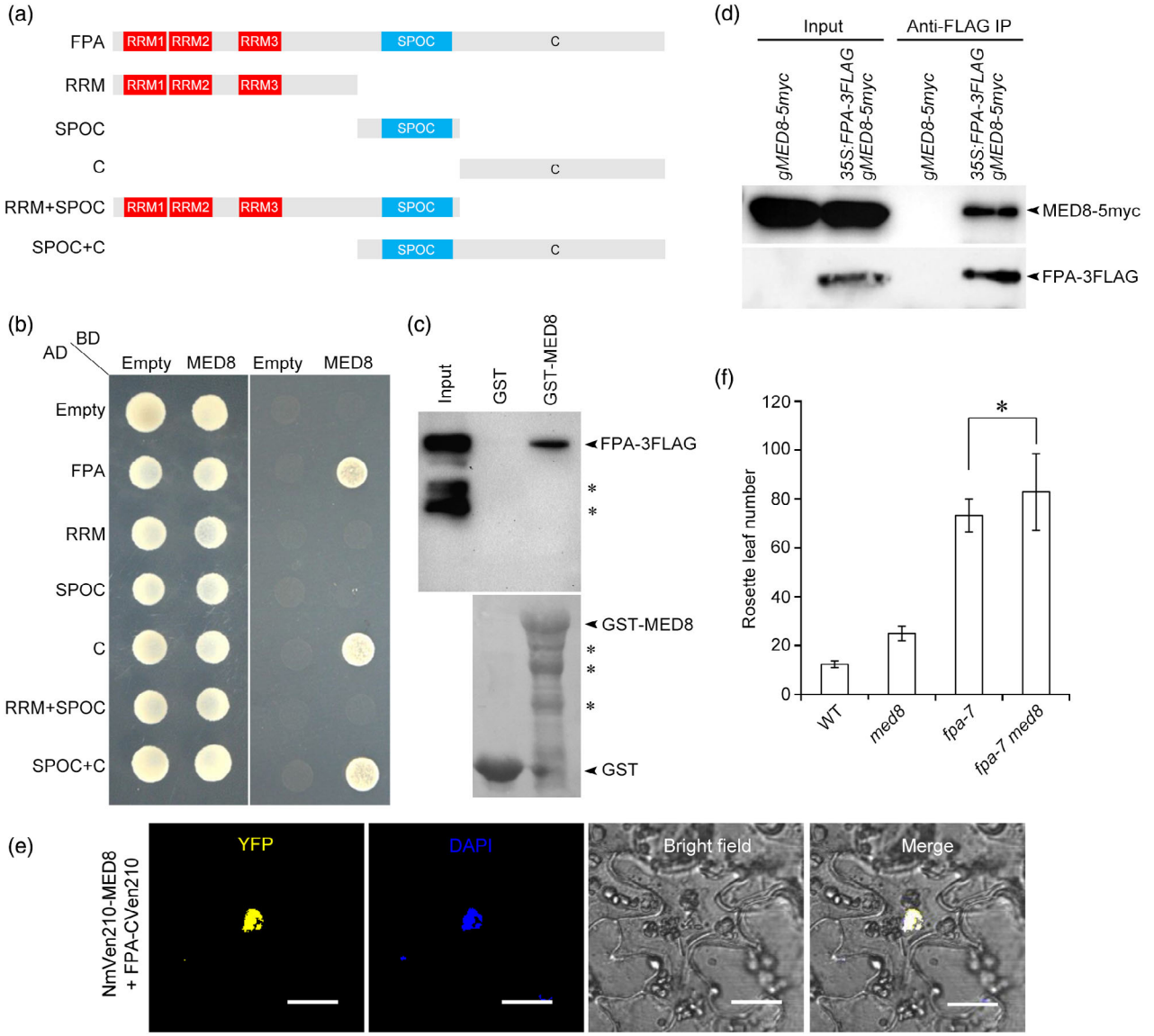

Figure 5. MED8 interacts with FPA.
(a) Top panel shows the schematic diagram of the FPA protein with N-terminal RNA recognition motifs (RRMs), a conserved SPEN paralog and ortholog C-terminal (SPOC) domain and a C-terminal region (C). (b) Yeast two-hybrid assay of the interaction between MED8 and FPA. Transformed yeast cells harboring various FPA truncated proteins fused to AD (activation domain) and MED8 fused to BD (binding domain) were grown on SD/-Leu/-Trp medium (left panel) and SD/-Ade/-His/-Leu/-Trp medium (right panel). (c) Semi-*in vivo* pull-down assay with MED8 and FPA. Whole-protein extract from *35S:FPA-3FLAG* transgenic plants was incubated with immobilized GST or GST–MED8. Immunoblot analysis was performed using anti-FLAG antibody. Input, 5% of the whole-protein extract. Asterisks indicate non-specific bands. (d) *In vivo* interaction between MED8 and FPA shown by co-immunoprecipitation in Arabidopsis. Total protein extracts from *gMED8-5myc* and *gMED8-5myc 35S:FPA-3FLAG* plants at 9 DAG were immunoprecipitated by anti-FLAG antibody. The input and coimmunoprecipitated proteins were detected by either anti-myc (upper panel) or anti-FLAG (middle panel) antibodies. The lower panel shows the Coomassie brilliant blue (CBB) staining of Rubisco as a loading control. (e) BiFC analysis of the interaction between MED8 and FPA in *N. benthamiana* leaf epidermal cells. Yellow fluorescence protein (YFP), fluorescence of yellow fluorescent protein; Merge, merge of YFP, DAPI and bright field. Scale bar: 20 μm. (f) Flowering time of *med8 fpa-7* under LD. Values were scored from at least 15 plants of each genotype. Asterisk indicates a significant difference in flowering time of *med8 fpa-7* compared with that of *fpa-7* ($P < 0.05$).

MED8 interacts with FPA

To clarify the effect of MED8 on floral transition, we performed yeast two-hybrid screening to discover MED8 interacting proteins and found that FPA was among the identified proteins. We used different approaches to validate the interaction between MED8 and FPA. First, yeast two-hybrid assays validated the interaction between MED8 and full-length FPA (Figure 5a,b; Figure S8). Moreover, we found that the truncated SPOC domain plus C terminal region and C terminal region alone of FPA was sufficient for

its interaction with MED8 (Figure 5a,b). Second, using a semi-*in vivo* pull-down assay, we found that MED8 protein was able to pull down FPA-3FLAG protein isolated from *35S:FPA-3FLAG* transgenic seedlings (Figure 5c). Third, the *in vivo* interaction between MED8-5myc and FPA-3FLAG during floral transition was confirmed by coimmunoprecipitation analysis (Figure 5d). Fourth, we introduced *35S:MED8-GFP* and *35S:FPA-mCherry* into the epidermal cells of *N. benthamiana* leaves and examined their subcellular localization. Both MED8-GFP and FPA-mCherry were localized in the nucleus, similar to the pattern observed with DAPI staining (Figure S9). Moreover, the interaction between MED8 and FPA in the nucleus was confirmed by BiFC analysis (Figure 5e; Figure S10). These findings indicated that MED8 and FPA interact within the nucleus *in vivo*. Interestingly, genetic analysis revealed that *fpa-7 med8* double mutants exhibited delayed flowering compared to each of their individual under long-day conditions (Figure 5f), implying that MED8 and FPA may also influence flowering through other independent targets.

MED8 facilitates the recruitment of FPA to the *FLC* locus

To further reveal the mechanism by which MED8 affects *FLC* expression, we investigated whether MED8 was associated with *FLC* chromatin by using chromatin immunoprecipitation analysis using the *med8 gMED8-3FLAG* transgenic line, in which *gMED8-3FLAG* successfully restored the delayed flowering phenotype of *med8* (Figure 1e). We designed 14 fragments covering the *FLC* locus (Figure 6a). ChIP results revealed that MED8-3FLAG was associated with the *FLC* locus at relatively high levels at fragments 4 and 5 and at low levels at fragments 10 and 11 (Figure 6b), whereas MED8-3FLAG did not bind to *FT* genomic region (Figure S11). This result suggests that MED8 is directly associated with the *FLC* locus and plays a role in repressing *FLC* expression. Meanwhile, we found that the association of MED8-FLAG to the *FLC* locus was not altered in the *fpa-7* background (Figure 6b). In contrast, by using the *fpa-7 gFPA-3FLAG* transgenic line, in which *gFPA-3FLAG* successfully rescued the delayed flowering of *fpa-7* (Figure S12), we found that binding of FPA-3FLAG to the *FLC* locus at fragment 9, 10, and 11 (Hornyik et al., 2010), was significantly reduced in *fpa-7 med8 gFPA-3FLAG* as compared to that in the *fpa-7 gFPA-3FLAG* background (Figure 6c). Consistently, we found that MED8, but not FPA, interacted with fragments 4, 5, 10, and 11 of the *FLC* genomic region in yeast one-hybrid assay (Figure S13). These results suggest that the binding of FPA to *FLC* is relied on the activity of MED8.

To further reveal the role of MED8 on FPA function, *FPA* overexpression transgenic lines (line #7) were introduced into *med8* mutant by genetic crossing. *med8 35S:FPA-FLAG* flowered later than *35S:FPA-FLAG*, but earlier than *med8* mutant (Figure 6d,e). Furthermore, *FLC* were significantly increased in *med8 35S:FPA-FLAG* as compared to those in *35S:FPA-FLAG*, but decreased in *med8 35S:FPA-FLAG* as compared to those in *med8* mutant (Figure 6f). These findings further support that the FPA function in regulating *FLC* requires the activity of MED8, but FPA may also affect this process through association with other components.

DISCUSSION

The floral transition is a pivotal and complex process in flowering plants, which is regulated by various external factors and internal signals forming a complex of flowering genetic pathways (Kim & Sung, 2014; Kinoshita & Richter, 2020; Shim et al., 2017; Song et al., 2015). Among these flowering pathways, the autonomous pathway controls flowering regardless of day length by repressing the expression of *FLC* (Cheng et al., 2017; Wu, Fang, et al., 2020). FPA, one of the autonomous pathway genes, correlates with the regulation of *FLC* expression and subsequently promotes flowering (Hornyik et al., 2010). However, the regulation of this process remains unclear. Here, we show that the regulation of *FLC* expression depends on MED8 and that MED8 recruits FPA to prevent the overproduction of *FLC* transcripts in Arabidopsis (Figure 7).

MED8 promotes flowering through *FLC*

Expression levels of *FLC*, *FT*, and *SOC1* were all altered in *med8* mutants compared to wild-type seedlings during the floral transition (Figure 4a–c), which is consistent with the delayed flowering phenotype of *med8*. Here, we have shown that the altered *FLC* expression level is the main reason for the late flowering of *med8*. First, *FRI med8* showed a similar flowering time to *FRI* (Figure 4d), suggesting that *MED8* acted in the same pathway as *FRI*. Second, *flc-3* almost fully suppressed the late flowering of *med8* under both long-day and short-day conditions (Figure 4d,e; Figure S6). Third, both *ft-10* and *soc1-2* enhanced the late-flowering phenotype of *med8* (Figure S7), and expression levels of *FT* and *SOC1* were restored in *flc-3 med8* double mutants as compared to that in *med8* mutants (Figure 4f). However, the effect of MED8 on *FT* expression is only partially dependent on *FLC*, as the *flc-3 med8* double mutant did not fully restore *FT* expression to that in the *flc-3* mutant (Figure 4f), indicating that MED8 may also control *FT* expression in an *FLC*-independent manner. Expression of two close homologs of *FLC*, *MAF4*, and *MAF5*, was also increased in *med8* seedlings (Figure S5a,b), and ChIP-qPCR assays indicated that MED8 also bound the *MAF5* locus (Figure S14), suggesting that the repressive effect of MED8 on *FT* expression may also be *MAF5* dependent. Transcriptomic analysis results showed that other flowering-related genes were also misregulated in *med8* mutants, such as *FDP*, *SPL3*, *SPL5*, *AGL19*, and *AGL24* (Dataset S2). As there

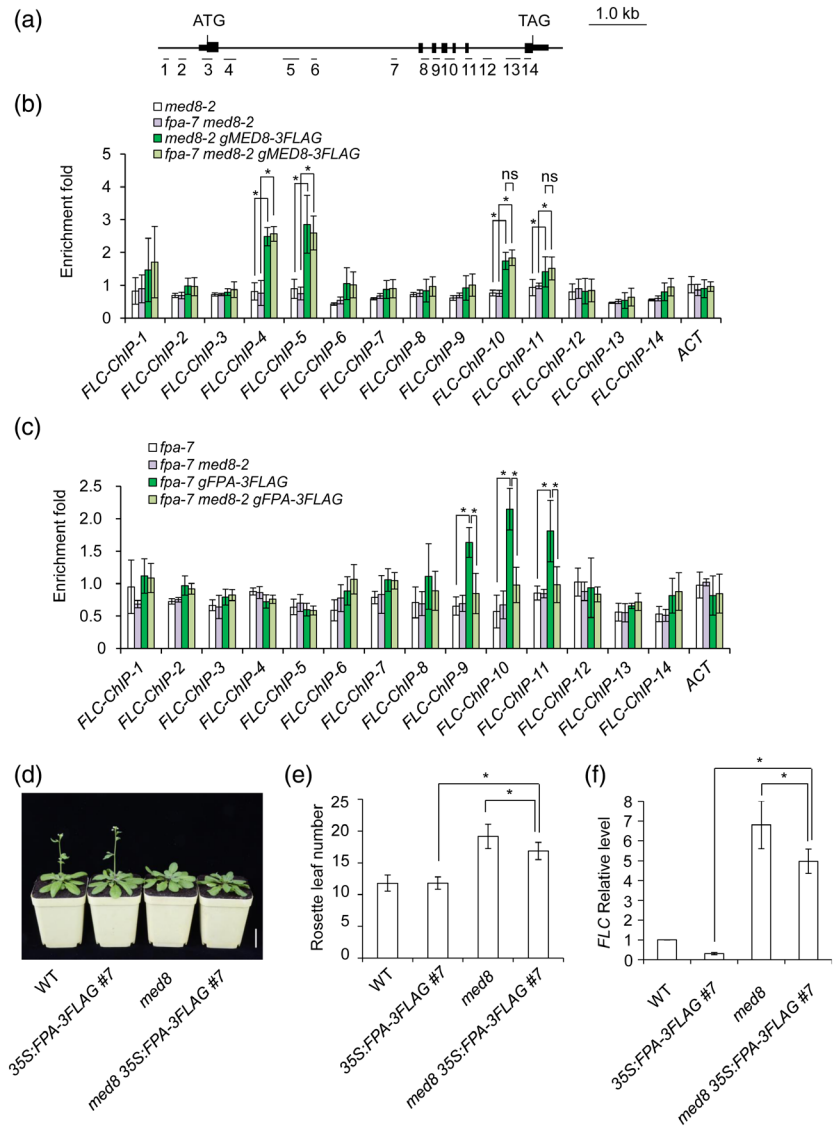

Figure 6. The function of FPA in flowering time requires MED8 activity to repress *FLC* expression.
(a) Schematic representation of *FLC* locus. Lines represent the DNA fragments amplified in ChIP analysis shown in (b, c). (b, c) ChIP analysis of MED8-3FLAG (b) and FPA-3FLAG (c) binding to the *FLC* genomic region in 9-day-old seedlings. Enrichment fold of each fragment was calculated first by normalizing the amount of a target DNA fragment against a genomic fragment of *TUB2* as an internal control. An *ACTIN* (*ACT*) fragment was amplified as a negative control. Error bars indicate SD of four biological replicates. Asterisks indicate significant differences of enrichment fold of the fragment (Student's *t* test, $P < 0.05$). (d) *med8 35S:FPA-FLAG* flowers later than *35S:FPA-FLAG* under long-day conditions. Scale bar, 2 cm. (e) Flowering time of wild-type, *35S:FPA-FLAG*, *med8* and *med8 35S:FPA-FLAG* grown under long-day conditions. Values were scored from at least 15 plants of each genotype. Error bars indicate SD. The asterisk indicates a significant difference in flowering time between *med8 35S:FPA-FLAG* and *35S:FPA-FLAG*, *med8 35S:FPA-FLAG* and *med8* (Student's *t* test, $P < 0.05$). (f) Expression of *FLC* in 9-day-old seedlings of wild-type, *35S:FPA-FLAG*, *med8* and *med8 35S:FPA-FLAG* grown under long days as determined by quantitative real-time PCR. All samples were collected at the end of long-day conditions (ZT16). The levels of gene expression normalized to *TUB2* expression are shown as relative values to that of wild-type set at 1. Error bars indicate SD for three independent PCR amplifications on three biological replicates. Asterisks indicate significant differences of *FLC* expression between *35S:FPA-FLAG* and *med8 35S:FPA-FLAG* plants, *med8* and *med8 35S:FPA-FLAG* plants (Student's *t* test, $P < 0.05$).

is intensive crosstalk among these flowering genes, the relationship between MED8 and the other flowering genes needs to be further elucidated.

MED8 prevents the overproduction of *FLC* transcripts

It has been shown that FPA regulates the expression of *FLC* in Arabidopsis (Hornyik et al., 2010; Liu et al., 2007; Liu et al., 2010), but the mechanism of how FPA regulates *FLC* expression is still largely unknown. We provide several lines of evidence that MED8 is involved in the regulation of *FLC* expression. First, ChIP-qPCR assays indicated that MED8 was recruited to the *FLC* locus. Second, the loss function of *MED8* resulted in excess amount of *FLC* expression, while the over-expression of *MED8* resulted in

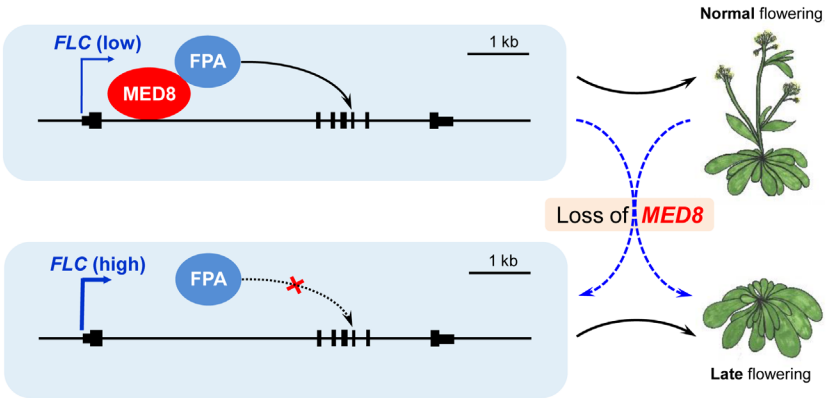

Figure 7. A working model describing regulation of flowering time by MED8.
When MED8 is present, it recruits FPA to prevent excessive *FLC* transcripts. When MED8 is absent, *FLC* transcripts are increased, thus precisely controlling the timing of floral transition in Arabidopsis.

reduced amount of *FLC* expression. Third, loss-function of *MED8* showed delay flowering under both long-day and short-day conditions (Figure 1c,d), and elevated *FLC* transcripts. Together, these findings ascribe a function of MED8 in preventing the overproduction of *FLC* transcripts. Therefore, MED8 is a novel regulator in the autonomous pathway and functions to prevent excessive *FLC* sense transcripts.

MED8 controls the recruitment of FPA to *FLC* locus

Several lines of evidence have demonstrated that MED8 interacts with FPA in regulating *FLC* sense transcripts. First, several protein–protein interaction assays indicated that MED8 interacts with FPA *in vivo* (Figure 5). Second, ChIP-qPCR assays demonstrated that FPA binding to *FLC* is dependent on the activity of MED8 (Figure 6c). Third, FPA's function in regulating flowering time and *FLC* requires the activity of MED8 (Figure 6d–f). Collectively, these findings indicate that MED8 has a crucial function in the recruitment of FPA to the *FLC* locus. Therefore, our results revealed that MED8 forms a complex with FPA to facilitate the regulation of *FLC* sense transcripts. In other words, the MED8-FPA complex functions to prevent excessive *FLC* transcripts.

Mediator has been reported to associate with promoter, coding, and terminator regions of target genes, as well as intergenic regions (Andrau et al., 2006; Hemsley et al., 2014; Lai et al., 2014; Wu, Deng, et al., 2020; Zhu et al., 2006). Furthermore, it has been reported that regulation of *FLC* expression involves coordination of transcription initiation with elongation (Li, Jiang, et al., 2018; Wu et al., 2016). It is possible that the MED8 and FPA complex regulates *FLC* expression by coordinating the changes in transcription initiation and elongation.

Split ends (Spen) family contains N-terminal RNA recognition motifs (RRMs) and a Spen paralogue and orthologue C-terminal (SPOC) domain (Arieti et al., 2014; Sanchez-Pulido et al., 2004; Zhang et al., 2016). FPA has been found to regulate *FLC* sense transcripts, which may be due to the function of the RRMs domain, but the molecular mechanism of SPOC domain remains unclear. We have shown that RRMs domain of FPA protein could not interact with MED8. But unexpectedly, the C-terminal region, rather than the SPOC domain of FPA that thought to be responsible for protein–protein interaction, is involved in FPA-MED8 interaction (Figure 5a). Further study should pay more attention to the structure of the FPA C-terminal region, as it could potentially have a significant impact on the interaction of Spen proteins.

MED8 and FPA may interact with other components in flowering

We have shown that MED8 plays a role in the recruitment of FPA to the *FLC* gene site to prevent excessive *FLC* sense transcripts. We speculate that MED8 and FPA may interact with other proteins to control the expression of *FLC* sense transcripts. First, ChIP-qPCR results have revealed that MED8 was not only associated with the *FLC* locus at fragments 10 and 11, as FPA was but also at fragments 4 and 5. Furthermore, the amount of MED8 at fragments 4 and 5 was relatively higher than that at fragment 10 (Figure 6b). These results suggest that MED8 may associate with other regulators, rather than FPA, at fragments 4 and 5. Second, genetic analysis showed that *fpa-7 med8* double mutants exhibited delayed flowering compared to each of their individual mutants under long-day conditions (Figure 5f), suggesting that MED8 may also associate with other autonomous pathway components such as *FCA* which also regulates the production of *FLC* sense RNAs (Liu et al., 2007; Liu et al., 2010) in preventing *FLC* sense transcripts. Furthermore, *fpa-7* flowered much later than *med8* (Figure 5f), while *med8 35S:FPA-FLAG* flowered earlier than *med8* mutant, and *FLC* was decreased in *med8 35S:FPA-FLAG* as compared to those in *med8* mutant (Figure 6f), implying that FPA may affect this process through

association with other components. Further studies should focus on investigating other associated proteins of MED8 or FPA that associate with regulation of *FLC* sense transcripts.

In conclusion, we have shown that the Mediator subunit MED8 represses *FLC* expression through facilitating the binding of FPA to the *FLC* locus to ensure appropriate timing of flowering for reproductive success. Since MED8 in other plant species has been isolated (Wang et al., 2011; Zhang et al., 2021), it will be interesting to explore if it also forms a complex with FPA to regulate flowering in other plant species. Moreover, in consideration of the conserved nature of Mediators in eukaryotes, our study sheds new light on the functional role of Mediator subunits in facilitating other important developmental processes in eukaryotes.

EXPERIMENTAL PROCEDURES

Plant materials and growth conditions

Plants were grown on soil under long-day conditions (16 h light, 8 h dark) or short-day conditions (8 h light, 16 h dark) at 23°C. The mutants *med8* (SALK_092406), *fpa-7* (SALK_138449), *gi-1*, *co-9*, *ft-10*, *soc1-2*, *svp-41*, Col:*FRI*^{SF2} (*FRI-Col*), *flc-3*, *fca-2*, *fld-3*, *flk-1* and *fve-4* are in the Col background. Transgenic plants of *35S:SVP* have been described previously[14]. *med8* (SALK_092406), *fpa-7* (SALK_138449) seeds were acquired from the Arabidopsis Biological Resource Center. *Agrobacterium tumefaciens*-mediated transformation was used to generate transgenic plants via floral dipping. Transformants containing *gMED8-3FLAG*, *35S:FPA-3FLAG*, *35S:MED8-GFP*, *gFPA-3FLAG*, and *pMED8-GUS* were selected on MS medium containing hygromycin.

Plasmid construction

To create *gMED8-FLAG* and *gFPA-3FLAG*, a 5.2-kb *MED8* genomic fragment (*gMED8*) and a 7.2-kb *FPA* genomic fragment (*gFPA*) were amplified, and the resulting PCR fragments were inserted into the binary vector pCAMBIA1300 which already contains a FLAG tag, respectively. *pMED8-GUS* was constructed by inserting the 2.4-kb 5′ upstream sequence of *MED8* into pCAMBIA1300-GUS. To construct *35S:MED8-GFP*, the coding sequence of *MED8* was cloned into pCAMBIA1300-35S-GFP. To construct *35S:MED8-5myc*, the coding sequence of *MED8* was cloned into pCAMBIA1300-35S-5myc. To construct *35S:FPA-FLAG*, the coding sequence of *FPA* was cloned into pCAMBIA1300-35S-FLAG. The primers used for plasmid construction are listed in Table S2.

Yeast two-hybrid assay

The coding regions of *MED8* and *FPA* and their truncated versions were amplified and cloned into pGADT7 or pGBKT7 (Clontech, Palo Alto, CA, USA). The Yeastmaker Yeast Transformation System 2 was used to perform the yeast two-hybrid assay according to the instructions provided by Clontech. All primers used for these constructs are listed in Table S2.

GST pull-down assay

To generate proteins with GST tags, the coding region of *MED8* was inserted into pGEX-4T-1 vector (Pharmacia, Piscataway, NJ, USA). This construct and pGEX-4T-1 vector were introduced into *E. coli* Rosetta (DE3) (Novagen, San Diego, CA, USA), and the expression of the protein was induced by IPTG. For subsequent pull-down assays, the soluble GST fusion proteins were extracted and immobilized onto glutathione sepharose beads (17-0756-01, Amersham Biosciences, Piscataway, NJ, USA).

To perform the semi-*in vivo* pull-down assay using Arabidopsis protein extracts, 9-day-old *gFPA-FLAG* seedlings grown on soil were collected and ground using liquid nitrogen. The extraction buffer (50 mM Tris–HCl pH 7.5, 150 mM NaCl, 1 mM EDTA, 5% glycerol, 0.5% Triton X-100, 1 mM PMSF, proteinase, and inhibitor cocktail) was used to extract total proteins. Protein extract was subsequently incubated with the immobilized GST and GST fusion proteins at 4°C for 2 h. It was then washed five times using 1 ml extraction buffer. The proteins remaining on the beads were separated using SDS-PAGE and identified using an anti-FLAG antibody (F-1804; Sigma-Aldrich, St. Louis, MO, USA; 1:2000 dilution).

Co-immunoprecipitation experiment

Nine-day-old seedlings were harvested and ground in liquid nitrogen. The extraction buffer (50 mM Tris–HCl pH 7.5, 150 mM NaCl, 1 mM EDTA, 5% glycerol, 0.5% Triton X-100, 1 mM PMSF, proteinase, and inhibitor cocktail) was used to extract the total proteins. Protein extracts were subsequently incubated with anti-FLAG agarose beads (A4596, Sigma) at 4°C for 2 h. It was then washed five times with extraction buffer. Immunoprecipitated proteins and total protein extracts as inputs were separated using SDS-PAGE and identified using an anti-myc antibody (SC40, Santa Cruz Biotechnology, Dallas, TX, USA; 1:2000 dilution) or anti-FLAG antibody (F1804, Sigma; 1:2000 dilution).

BiFC analysis

The cDNAs were cloned into pDOE-03 vector containing N- and C-terminal yellow fluorescence protein mVenus for BiFC analysis as previously published (Gookin & Assmann, 2014). Briefly, the coding sequence of *MED8* was inserted into pDOE-03-NmVen210 to construct *pDOE-03-NmVen210-MED8*, and the coding sequence of *FPA* was inserted into pDOE-03-CVen210 to construct *pDOE-03-FPA-CVen210*. The combinations of NmVen210-MED8 + CVen210 and NmVen210 + FPA-CVen210 were used as negative controls for BiFC analysis. Primers used for these plasmids are listed in Table S2.

Expression analysis

RNA extraction was performed using the RNAprep Pure Plant Kit (Tiangen Biotech, Beijing, China) and cDNA synthesis was performed using M-MLV Reverse Transcriptase (Promega, Madison, WI, USA) following the manufacturers' instructions. The CFX96 or CFX384 real-time PCR detection system (Bio-Rad, Hercules, CA, USA) was used for quantitative real-time PCR with iQ SYBR Green Supermix (Bio-Rad). *TUBULIN 2* (*TUB2*) was used as the internal control for expression. The ΔCt method, as previously described by Liu et al. (2007), was used to calculate the relative expression levels of genes. Three biological replicates were performed for expression analysis. All primers used for gene expression analysis are listed in Table S2.

GUS staining

The GUS staining procedure was conducted according to the protocol published by Li, Zhang, et al. (2018) with slight modifications. Seedlings were treated with a staining solution containing GUS (100 mM sodium phosphate buffer, pH 7.0, 10 mM Ethylenediaminetetraacetic acid disodium salt, pH 8.0, 1 mM potassium ferrocyanide, 1 mM potassium ferricyanide, 0.5% (v/v) Triton X-100, 20% (v/v) methanol, and 0.5 mg ml^{-1} X-Gluc) using vacuum infiltration. They were then incubated with the same solution at 37°C for 6 h. The stained tissues were then subjected to an ethanol

series to remove chlorophyll. Finally, the tissues were placed in a clear solution (chloral hydrate/water/glycerol = 8 g/3 ml/1 ml) and observed under a light microscope.

ChIP assay

ChIP assays were conducted following the methods described previously (Shen et al., 2014). Nine-day-old seedlings (0.5 g) were collected and then fixed by 1% formaldehyde, and chromatin was extracted and sonicated to generate DNA fragments ranging from 200 to 500 bp. Anti-FLAG M2-Agarose (Sigma) was used to immunoprecipitate the sonicated chromatins. The DNA fragments that were precipitated were then recovered and analyzed by qPCR analysis using specific primers (Table S2) and SYBR Premix ExTaq Mix (Takara Bio, Otsu, Shiga, Japan). The relative fold increase was determined by comparing the amount of a specific DNA fragment to that of a *TUB2* or *ACTIN* genomic fragment and then normalizing it against the corresponding input DNA samples.

Transcriptome analysis

The isolation of total RNA from seedlings of both wild-type and *med8* mutant was carried out according to the method described above. The RNA-seq library was prepared following the instructions and sequenced using the BGIseq500 platform (BGI-Shenzhen, Shenzhen, China). Differentially expressed genes were determined by applying criteria of $|\log2(\text{fold-change})| > 1$ and a *q*-value <0.05. The transcriptome data have been submitted to NCBI (accession number PRJNA937467).

Yeast one-hybrid assay

The yeast one-hybrid assay was conducted utilizing the Matchmaker Gold Yeast One-Hybrid Library Screening System (Clontech, Palo Alto, CA, USA) and Yeastmaker Yeast Transformation System2 (Clontech). The fragments of *FLC* were cloned into the *pAbAi* vector. Different combinations of the plasmids *pAbAi-FLC* and *pGADT7-MED8* or *pGADT7-FPA* were transformed into yeast strain Y1HGold and grown on SD medium lacking Ura with either 0 or 100 ng ml^{-1} AbA at 30°C for 3 days. All primers used are listed in Table S2.

ACKNOWLEDGMENTS

This work was supported by grants from the National Natural Science Foundation of China (31770344 and 31970328 to C. Qin), the Agency for Science, Technology and Research (A*STAR) under its Industry Alignment Fund - Pre Positioning (IAF-PP) (A19D9a0096 to L. Shen), and the intramural resource support from Temasek Life Sciences Laboratory (L. Shen).

AUTHOR CONTRIBUTIONS

CY, HY, LS, and CQ conceived and designed the study. CY, YH, QL, JX, WZ, and LS performed the experiments. CY, YH, JX, WZ, HY, LS, and CQ analyzed data. HY, LS, and CQ wrote the paper. All authors read and approved the manuscript.

CONFLICT OF INTEREST STATEMENT

The authors declare no conflict of interest.

DATA AVAILABILITY STATEMENT

All relevant data can be found within the manuscript and its supporting materials.

SUPPORTING INFORMATION

Additional Supporting Information may be found in the online version of this article.

Dataset S1. Differentially expressed genes in *med8* mutant.

Dataset S2. Expression level of flowering genes in *med8* mutant.

Dataset S3. Expression of autonomous pathway regulators in *med8* mutant.

Figure S1. MED8 expression in two separate *med8 gMED8-3FLAG* transgenic lines.

Figure S2. Overexpression of *MED8* shows normal flowering phenotype under long-day conditions.

Figure S3. *MED8* expression levels do not exhibit an obvious diurnal oscillation pattern within a 24-h cycle under long-day conditions.

Figure S4. Transcriptional profiles of wild-type and *med8* mutant seedlings.

Figure S5. Temporal expression of *MAF4* (a), *MAF5* (b), and *SVP* (c) in developing wild-type (WT) and *med8* seedlings grown under long-day conditions determined by quantitative real-time PCR.

Figure S6. Flowering time of various mutants grown under long-day (a) and short-day (b) conditions.

Figure S7. Flowering time of various mutants grown under long-day conditions.

Figure S8. Yeast two-hybrid assay of the interaction between MED8 and FPA.

Figure S9. Coexpression of *35S:FPA-mCherry* and *35S:MED8-GFP* in *N. benthamiana* leaf epidermal cells.

Figure S10. Negative controls for BiFC analysis of the interaction between MED8 and FPA in *N. benthamiana* leaf epidermal cells.

Figure S11. MED8 is not associated with the *FT* locus.

Figure S12. *gFPA-3FLAG* fully rescues the late-flowering time of *fpa-7* mutants.

Figure S13. Yeast one-hybrid assay of the interaction between MED8 or FPA and the fragments of *FLC*.

Figure S14. MED8 is associated with the *MAF5* locus.

Table S1. The sequence of the T-DNA (SALK_092406) insertion site.

Table S2. List of primers used in this study.

REFERENCES

Abou-Elwafa, S.F., Büttner, B., Chia, T., Schulze-Buxloh, G., Hohmann, U., Mutasa-Göttgens, E. *et al.* (2011) Conservation and divergence of autonomous pathway genes in the flowering regulatory network of Beta vulgaris. *Journal of Experimental Botany*, **62**, 3359–3374.

Amasino, R.M. & Michaels, S.D. (2010) The timing of flowering. *Plant Physiology*, **154**, 516–520.

Andrau, J.C., van de Pasch, L., Lijnzaad, P., Bijma, T., Koerkamp, M.G., van de Peppel, J. *et al.* (2006) Genome-wide location of the coactivator mediator: binding without activation and transient Cdk8 interaction on DNA. *Molecular Cell*, **22**, 179–192.

Andres, F. & Coupland, G. (2012) The genetic basis of flowering responses to seasonal cues. *Nature Reviews. Genetics*, **13**, 627–639.

Arieti, F., Gabus, C., Tambalo, M., Huet, T., Round, A. & Thore, S. (2014) The crystal structure of the split end protein SHARP adds a new layer of complexity to proteins containing RNA recognition motifs. *Nucleic Acids Research*, **42**, 6742–6752.

Ausin, I., Alonso-Blanco, C., Jarillo, J.A., Ruiz-Garcia, L. & Martinez-Zapater, J.M. (2004) Regulation of flowering time by FVE, a retinoblastoma-associated protein. *Nature Genetics*, **36**, 162–166.

Cheng, J.Z., Zhou, Y.P., Lv, T.X., Xie, C.P. & Tian, C.E. (2017) Research progress on the autonomous flowering time pathway in Arabidopsis. *Physiology and Molecular Biology of Plants*, **23**, 477–485.

Duc, C., **Sherstnev, A.**, **Cole, C.**, **Barton, G.J.** & **Simpson, G.G.** (2013) Transcription termination and chimeric RNA formation controlled by Arabidopsis thaliana FPA. *PLoS Genetics*, **9**, e1003867.

Fallath, T., **Kidd, B.N.**, **Stiller, J.**, **Davoine, C.**, **Bjorklund, S.**, **Manners, J.M.** ***et al.*** (2017) MEDIATOR18 and MEDIATOR20 confer susceptibility to fusarium oxysporum in Arabidopsis thaliana. *PLoS One*, **12**, e0176022.

Gookin, T.E. & **Assmann, S.M.** (2014) Significant reduction of BiFC non-specific assembly facilitates in planta assessment of heterotrimeric G-protein interactors. *The Plant Journal*, **80**, 553–567.

Guo, J., **Wei, L.**, **Chen, S.S.**, **Cai, X.W.**, **Su, Y.N.**, **Li, L.** ***et al.*** (2021) The CBP/p300 histone acetyltransferases function as plant-specific MEDIATOR subunits in Arabidopsis. *Journal of Integrative Plant Biology*, **63**, 755–771.

Hammoudi, V. (2021) Oxidative stress is H_2O_2 under the bridge without MED8. *Plant Cell*, **33**, 1855–1856.

He, H., **Denecker, J.**, **Van Der Kelen, K.**, **Willems, P.**, **Pottie, R.**, **Phua, S.Y.** ***et al.*** (2021) The Arabidopsis mediator complex subunit 8 regulates oxidative stress responses. *Plant Cell*, **0**, 1–26.

He, Y. (2009) Control of the transition to flowering by chromatin modifications. *Molecular Plant*, **2**, 554–564.

He, Y. (2012) Chromatin regulation of flowering. *Trends in Plant Science*, **17**, 556–562.

He, Y., **Michaels, S.D.** & **Amasino, R.M.** (2003) Regulation of flowering time by histone acetylation in *Arabidopsis*. *Science*, **302**, 1751–1754.

Hemsley, P.A., **Hurst, C.H.**, **Kaliyadasa, E.**, **Lamb, R.**, **Knight, M.R.**, **De Cothi, E.A.** ***et al.*** (2014) The Arabidopsis mediator complex subunits MED16, MED14, and MED2 regulate mediator and RNA polymerase II recruitment to CBF-responsive cold-regulated genes. *Plant Cell*, **26**, 465–484.

Hepworth, S.R., **Valverde, F.**, **Ravenscroft, D.**, **Mouradov, A.** & **Coupland, G.** (2002) Antagonistic regulation of flowering-time gene SOC1 by CONSTANS and FLC via separate promoter motifs. *The EMBO Journal*, **21**, 4327–4337.

Hornyik, C., **Terzi, L.C.** & **Simpson, G.G.** (2010) The spen family protein FPA controls alternative cleavage and polyadenylation of RNA. *Developmental Cell*, **18**, 203–213.

Kidd, B.N., **Edgar, C.I.**, **Kumar, K.K.**, **Aitken, E.A.**, **Schenk, P.M.**, **Manners, J.M.** ***et al.*** (2009) The mediator complex subunit PFT1 is a key regulator of jasmonate-dependent defense in Arabidopsis. *Plant Cell*, **21**, 2237–2252.

Kim, D.H. & **Sung, S.** (2010) The plant homeo domain finger protein, VIN3-LIKE 2, is necessary for photoperiod-mediated epigenetic regulation of the floral repressor, MAF5. *Proceedings of the National Academy of Sciences of the United States of America*, **107**, 17029–17034.

Kim, D.H. & **Sung, S.** (2014) Genetic and epigenetic mechanisms underlying vernalization. *The Arabidopsis Book/American Society of Plant Biologists*, **12**, e0171.

Kim, H.J., **Hyun, Y.**, **Park, J.Y.**, **Park, M.J.**, **Park, M.K.**, **Kim, M.D.** ***et al.*** (2004) A genetic link between cold responses and flowering time through *FVE* in *Arabidopsis thaliana*. *Nature Genetics*, **36**, 167–171.

Kinoshita, A. & **Richter, R.** (2020) Genetic and molecular basis of floral induction in Arabidopsis thaliana. *Journal of Experimental Botany*, **71**, 2490–2504.

Koornneef, M., **Hanhart, C.J.** & **van der Veen, J.H.** (1991) A genetic and physiological analysis of late flowering mutants in Arabidopsis thaliana. *Molecular & General Genetics*, **229**, 57–66.

Lai, Z., **Schluttenhofer, C.M.**, **Bhide, K.**, **Shreve, J.**, **Thimmapuram, J.**, **Lee, S.Y.** ***et al.*** (2014) MED18 interaction with distinct transcription factors regulates multiple plant functions. *Nature Communications*, **5**, 3064.

Lee, I., **Aukerman, M.J.**, **Gore, S.L.**, **Lohman, K.N.**, **Michaels, S.D.**, **Weaver, L.M.** ***et al.*** (1994) Isolation of *LUMINIDEPENDENS*: a gene involved in the control of flowering time in Arabidopsis. *Plant Cell*, **6**, 75–83.

Li, C., **Zhang, B.**, **Chen, B.**, **Ji, L.** & **Yu, H.** (2018) Site-specific phosphorylation of TRANSPARENT TESTA GLABRA1 mediates carbon partitioning in Arabidopsis seeds. *Nature Communications*, **9**, 571.

Li, X., **Yang, R.** & **Chen, H.** (2018) The Arabidopsis thaliana Mediator subunit MED8 regulates plant immunity to *Botrytis cinerea* through interacting with the basic helix-loop-helix (bHLH) transcription factor FAMA. *PLoS One*, **13**, e0193458.

Li, Z., **Jiang, D.** & **He, Y.** (2018) FRIGIDA establishes a local chromosomal environment for FLOWERING LOCUS C mRNA production. *Nature Plants*, **4**, 836–846.

Lim, M.H., **Kim, J.**, **Kim, Y.S.**, **Chung, K.S.**, **Seo, Y.H.**, **Lee, I.** ***et al.*** (2004) A new Arabidopsis gene, *FLK*, encodes an RNA binding protein with K homology motifs and regulates flowering time via *FLOWERING LOCUS C*. *Plant Cell*, **16**, 731–740.

Liu, F., **Marquardt, S.**, **Lister, C.**, **Swiezewski, S.** & **Dean, C.** (2010) Targeted 3′ processing of antisense transcripts triggers Arabidopsis FLC chromatin silencing. *Science*, **327**, 94–97.

Liu, F., **Quesada, V.**, **Crevillen, P.**, **Baurle, I.**, **Swiezewski, S.** & **Dean, C.** (2007) The Arabidopsis RNA-binding protein FCA requires a lysine-specific demethylase 1 homolog to downregulate FLC. *Molecular Cell*, **28**, 398–407.

Macknight, R., **Bancroft, I.**, **Page, T.**, **Lister, C.**, **Schmidt, R.**, **Love, K.** ***et al.*** (1997) *FCA*, a gene controlling flowering time in Arabidopsis, encodes a protein containing RNA-binding domains. *Cell*, **89**, 737–745.

Mahrez, W., **Shin, J.**, **Munoz-Viana, R.**, **Figueiredo, D.D.**, **Trejo-Arellano, M.S.**, **Exner, V.** ***et al.*** (2016) BRR2a affects flowering time via FLC splicing. *PLoS Genetics*, **12**, e1005924.

Marquardt, S. (2006) Additional targets of the *Arabidopsis* autonomous pathway members, FCA and FY. *Journal of Experimental Botany*, **57**, 3379–3386.

Michaels, S.D. (2009) Flowering time regulation produces much fruit. *Current Opinion in Plant Biology*, **12**, 75–80.

Mockler, T.C., **Yu, X.**, **Shalitin, D.**, **Parikh, D.**, **Michael, T.P.**, **Liou, J.** ***et al.*** (2004) Regulation of flowering time in *Arabidopsis* by K homology domain proteins. *Proceedings of the National Academy of Sciences of the United States of America*, **101**, 12759–12764.

Mouradov, A., **Cremer, F.** & **Coupland, G.** (2002) Control of flowering time: interacting pathways as a basis for diversity. *Plant Cell*, **14**, S111–S130.

Parenicova, L., **de Folter, S.**, **Kieffer, M.**, **Horner, D.S.**, **Favalli, C.**, **Busscher, J.** ***et al.*** (2003) Molecular and phylogenetic analyses of the complete MADS-box transcription factor family in Arabidopsis: new openings to the MADS world. *Plant Cell*, **15**, 1538–1551.

Pose, D., **Verhage, L.**, **Ott, F.**, **Yant, L.**, **Mathieu, J.**, **Angenent, G.C.** ***et al.*** (2013) Temperature-dependent regulation of flowering by antagonistic FLM variants. *Nature*, **503**, 414–417.

Quesada, V., **Macknight, R.**, **Dean, C.** & **Simpson, G.G.** (2003) Autoregulation of *FCA* pre-mRNA processing controls *Arabidopsis* flowering time. *The EMBO Journal*, **22**, 3142–3152.

Rataj, K. & **Simpson, G.G.** (2014) Message ends: RNA 3′ processing and flowering time control. *Journal of Experimental Botany*, **65**, 353–363.

Ratcliffe, O.J., **Nadzan, G.C.**, **Reuber, T.L.** & **Riechmann, J.L.** (2001) Regulation of flowering in Arabidopsis by an FLC homologue. *Plant Physiology*, **126**, 122–132.

Sanchez-Pulido, L., **Rojas, A.M.**, **van Wely, K.H.**, **Martinez, A.C.** & **Valencia, A.** (2004) SPOC: a widely distributed domain associated with cancer, apoptosis and transcription. *BMC Bioinformatics*, **5**, 91.

Schomburg, F.M., **Patton, D.A.**, **Meinke, D.W.** & **Amasino, R.M.** (2001) FPA, a gene involved in floral induction in Arabidopsis, encodes a protein containing RNA-recognition motifs. *Plant Cell*, **13**, 1427–1436.

Searle, I., **He, Y.**, **Turck, F.**, **Vincent, C.**, **Fornara, F.**, **Krober, S.** ***et al.*** (2006) The transcription factor FLC confers a flowering response to vernalization by repressing meristem competence and systemic signaling in Arabidopsis. *Genes & Development*, **20**, 898–912.

Seguela-Arnaud, M., **Smith, C.**, **Uribe, M.C.**, **May, S.**, **Fischl, H.**, **McKenzie, N.** ***et al.*** (2015) The mediator complex subunits MED25/PFT1 and MED8 are required for transcriptional responses to changes in cell wall arabinose composition and glucose treatment in Arabidopsis thaliana. *BMC Plant Biology*, **15**, 215.

Shen, L., **Thong, Z.**, **Gong, X.**, **Shen, Q.**, **Gan, Y.** & **Yu, H.** (2014) The putative PRC1 RING-finger protein AtRING1A regulates flowering through repressing MADS AFFECTING FLOWERING genes in Arabidopsis. *Development*, **141**, 1303–1312.

Shim, J.S., **Kubota, A.** & **Imaizumi, T.** (2017) Circadian clock and photoperiodic flowering in Arabidopsis: CONSTANS is a hub for signal integration. *Plant Physiology*, **173**, 5–15.

Simpson, G.G. & **Dean, C.** (2002) Arabidopsis, the Rosetta stone of flowering time? *Science*, **296**, 285–289.

Simpson, G.G., **Dijkwel, P.P.**, **Quesada, V.**, **Henderson, I.** & **Dean, C.** (2003) FY is an RNA 3′ end-processing factor that interacts with FCA to control the *Arabidopsis* floral transition. *Cell*, **113**, 777–787.

Song, Y.H., **Shim, J.S.**, **Kinmonth-Schultz, H.A.** & **Imaizumi, T.** (2015) Photoperiodic flowering: time measurement mechanisms in leaves. *Annual Review of Plant Biology*, **66**, 441–464.

Srikanth, A. & **Schmid, M.** (2011) Regulation of flowering time: all roads lead to Rome. *Cellular and Molecular Life Sciences*, **68**, 2013–2037.

Wang, F., **Wei, H.**, **Tong, Z.**, **Zhang, X.**, **Yang, Z.**, **Lan, T.** ***et al.*** (2011) Knockdown of NtMed8, a Med8-like gene, causes abnormal development of vegetative and floral organs in tobacco (*Nicotiana tabacum* L.). *Plant Cell Reports*, **30**, 2117–2129.

Wigge, P.A. (2013) Ambient temperature signalling in plants. *Current Opinion in Plant Biology*, **16**, 661–666.

Wu, F., **Deng, L.**, **Zhai, Q.**, **Zhao, J.**, **Chen, Q.** & **Li, C.** (2020) Mediator subunit MED25 couples alternative splicing of JAZ genes with fine-tuning of jasmonate signaling. *Plant Cell*, **32**, 429–448.

Wu, Z., **Fang, X.**, **Zhu, D.** & **Dean, C.** (2020) Autonomous pathway: FLOWERING LOCUS C repression through an antisense-mediated chromatin-silencing mechanism. *Plant Physiology*, **182**, 27–37.

Wu, Z., **Ietswaart, R.**, **Liu, F.**, **Yang, H.**, **Howard, M.** & **Dean, C.** (2016) Quantitative regulation of *FLC* via coordinated transcriptional initiation and elongation. *Proceedings of the National Academy of Sciences of the United States of America*, **113**, 218–223.

Xu, R. & **Li, Y.** (2012) The mediator complex subunit 8 regulates organ size in Arabidopsis thaliana. *Plant Signaling & Behavior*, **7**, 182–183.

Yan, Y., **Shen, L.**, **Chen, Y.**, **Bao, S.**, **Thong, Z.** & **Yu, H.** (2014) A MYB-domain protein EFM mediates flowering responses to environmental cues in Arabidopsis. *Developmental Cell*, **30**, 437–448.

Yang, Y., **Li, L.** & **Qu, L.J.** (2016) Plant mediator complex and its critical functions in transcription regulation. *Journal of Integrative Plant Biology*, **58**, 106–118.

Yu, X. & **Michaels, S.D.** (2010) The Arabidopsis Paf1c complex component CDC73 participates in the modification of *FLOWERING LOCUS C* chromatin. *Plant Physiology*, **153**, 1074–1084.

Zhang, L., **Song, Y.**, **Liu, K.** & **Gong, F.** (2021) The tomato mediator subunit MED8 positively regulates plant response to *Botrytis cinerea*. *Journal of Plant Physiology*, **266**, 153533.

Zhang, X., **Zhou, W.**, **Chen, Q.**, **Fang, M.**, **Zheng, S.**, **Scheres, B.** ***et al.*** (2018) Mediator subunit MED31 is required for radial patterning of Arabidopsis roots. *Proceedings of the National Academy of Sciences of the United States of America*, **115**, E5624–E5633.

Zhang, Y., **Rataj, K.**, **Simpson, G.G.** & **Tong, L.** (2016) Crystal structure of the SPOC domain of the Arabidopsis flowering regulator FPA. *PLoS One*, **11**, e0160694.

Zhu, X., **Wirén, M.**, **Sinha, I.**, **Rasmussen, N.N.**, **Linder, T.**, **Holmberg, S.** ***et al.*** (2006) Genomewide occupancy profile of mediator and the Srb8-11 module reveals interactions with coding regions. *Molecular Cell*, **22**, 169–178.